Spin waves in perpendicularly magnetized Co/Ni(111) multilayers in the presence of magnetic domains

G. Gubbiotti,[1,2] G. Carlotti,[2,3] S. Tacchi,[2] M. Madami,[2] T. Ono,[4] T. Koyama,[4] D. Chiba,[4] F. Casoli,[5] and M. G. Pini[6]

[1]*Istituto Officina dei Materiali del CNR (CNR-IOM), Unità di Perugia, c/o Dipartimento di Fisica, Università di Perugia, I-06123 Perugia, Italy*

[2]*CNISM, Unità di Perugia and Dipartimento di Fisica, Università di Perugia, I-06123 Perugia, Italy*

[3]*Centro S3, c/o Istituto Nanoscienze del CNR (CNR-NANO), I-41125 Modena, Italy*

[4]*Laboratory of Nano Spintronics, Division of Materials Chemistry, Istitute for Chemical Research, Kyoto University, Uji, Kyoto 611-0011, Japan*

[5]*Istituto Materiali per Elettronica e Magnetismo del CNR (CNR-IMEM), I-43124 Parma, Italy*

[6]*Istituto dei Sistemi Complessi del CNR (CNR-ISC), Unità di Firenze, I-50019 Sesto Fiorentino (FI), Italy*

(Received 13 March 2012; revised manuscript received 6 June 2012; published 5 July 2012)

Co/Ni(111) multilayers with variable cobalt thickness t_{Co} between 0.15 and 0.35 nm and fixed nickel thickness $t_{Ni} = 0.6$ nm were grown on a Pt(1.6 nm)/Ta(3 nm) substrate by dc magnetron sputtering. A strong perpendicular magnetic anisotropy was found both using vibrating sample magnetometry and Brillouin light scattering from thermally excited spin waves. The simultaneous presence of two spin-wave modes, for a range of magnetic fields H applied in plane between ≈2.5 and 5 kOe, was connected with the presence of bubble domains, revealed by polar Kerr microscopy. The lower frequency mode ($\nu \approx 3$ GHz), which exhibits a smooth dependence on the strength of H, was attributed to harmonic oscillations of the domain walls. The higher frequency mode, which displayed the typical field behavior of a film with a perpendicular anisotropy, was interpreted as the superposition of two nearly degenerate modes, associated, respectively, with the in-phase and out-of-phase precession of the spins in the bubble array. The higher frequency mode also displayed an unprecedented, nonmonotonic dependence *on cobalt thickness*, reflecting the nonmonotonic t_{Co} dependence of the effective anisotropy field of the multilayer.

DOI: 10.1103/PhysRevB.86.014401 PACS number(s): 75.70.Cn, 78.35.+c, 75.30.Ds, 75.60.Ej

I. INTRODUCTION

The search for magnetic multilayers with a strong perpendicular magnetic anisotropy (PMA) at room temperature has attracted much interest for the past two decades, owing to potential applications to high-density magnetic recording[1] and, more recently, to spintronic devices based on spin transfer torque effects.[2–11] Perpendicular anisotropy in the free layer of a spin torque oscillator was also shown[12] to be of crucial importance for the excitation of a dissipative droplet soliton (a highly nonuniform precessional state representing the dynamic, dissipative version of the "magnon droplet"[13,14]). Co/Ni(111) multilayers with PMA[15–18] appear to be quite interesting with respect to such spintronic devices since they are able to provide low values for the switching current ($I_c \approx 10^2$ μA) while maintaining large thermal stability.[19–23] Using a magnetic metal, like Ni, in lieu of a nonmagnetic noble metal, as a substrate for Co, is well known[15,16] to provide a wider range of cobalt thicknesses for which PMA can be observed in a multilayer, since the saturation magnetization of Ni is nearly three times smaller than that of Co. Quite recently, the role of Ta/Pt as an underlayer, acting as a template capable of promoting the fcc (111) orientation in Co/Ni films, deposited by dc magnetron sputtering onto Si substrates covered with SiO_2, was recently investigated.[24] It resulted that a Ta(3 nm)/Pt(1.2–4.8 nm) layer provides perpendicular magnetization of Co/Ni(111) multilayers, and the electrical resistivity of Ta/Pt is larger compared with that of the Co/Ni stack, so that small driving currents are required by the device.[24]

In this paper, we report on the analysis of the static and dynamical magnetic properties of Co/Ni multilayers grown with fcc (111) orientation by dc magnetron sputtering. The samples had the following structure: Pt(2 nm)/[Co(t_{Co})/Ni(0.6 nm)]$_{\times 4}$/Co(t_{Co})/Pt(1.6 nm)/Ta(3 nm)/substrate; that is, the stack was characterized by variable cobalt thickness (0.15 nm $\leqslant t_{Co} \leqslant$ 0.35 nm), Pt(1.6 nm)/Ta(3 nm) as buffer layer, and Pt(2 nm) as cap layer. Details about sample growth can be found in Refs. 4–9 and 24. Spin waves have been studied by Brillouin light scattering (BLS), which relies upon the inelastic scattering of light by thermal spin waves. It allows local measurements (the probed area is a circle with diameter of ≈30 μm) and has been exploited in the past to analyze spin waves in films and multilayers with PMA.[25–31] In some of the above cases[25,26] it was observed that, on reducing the strength of the magnetic field applied in plane, the spin-wave frequency decreases following a nearly linear law, reaches a minimum at a critical field H_C, and then increases again as the applied field is reduced to zero. This behavior was successfully interpreted as due to the reorientation of the magnetization, assumed to be uniform across the layers. In other cases,[27–31] however, the mode softening predicted by theory was not observed, and the spin-wave frequency continued to follow an almost linear decrease with the magnetic field, although with a smaller slope. In such cases, the presence of magnetic domains was invoked as the possible cause of the anomaly, even though neither a direct imaging of domains as a function of the field nor a quantitative reproduction of the experimental results was provided. Therefore, the problem of a quantitative understanding of the spin-wave behavior in multilayers with PMA during the reorientation transition and in presence of magnetic domains needs to be further investigated. The paper is organized as follows. In Sec. II we present the

experimental results, obtained by three different techniques, in the Co/Ni(111) multilayers. Section III is devoted to presenting a model for the interpretation of experimental BLS data, as well as theoretical results for the H and t_{Co} dependence of the various frequency modes. Finally, the conclusions are drawn in Sec. IV.

II. EXPERIMENTAL RESULTS

A. Hysteresis curves measured by vibrating sample magnetometry

The magnetization curves of the Co/Ni multilayers, measured at room temperature by a vibrating sample magnetometer (VSM) for magnetic field perpendicular and parallel to the film plane, are shown in Figs. 1(a) and 1(b), respectively. The sweep range was [−400, 400] Oe for perpendicular field and [−8000, 8000] Oe for in-plane field; the sweep speed was 80 Oe/s for perpendicular field and 250 Oe/s for in-plane field. The sample size was 10 × 10 mm. In the case of field applied perpendicular to the plane, the square shape of the VSM loops signals that the normal to the film is the easy direction. In these polar loops, the increase in coercive field, from 115 to 150 Oe upon increasing the cobalt layer thickness, signals the increase in the perpendicular anisotropy, stabilizing the out-of-plane orientation of the magnetization. For field applied parallel to the film plane, the loops have an S shape. In these longitudinal loops, the increase in the perpendicular anisotropy is signaled by the increase in the value of the saturation field H_{sat} as t_{Co} increases. An estimate of the effective out-of-plane anisotropy K_u^{eff} can be obtained, through a best fit procedure,[24,32] using the customary relationship $K_u^{eff} = \frac{1}{2} M_s (H_{sat} + 4\pi M_s)$, where M_s is the saturation magnetization of the multilayer. In the present samples, K_u^{eff} is estimated to range between ≈4.7 and 6.4×10^6 erg/cm^3. (We use the convention that the out-of-plane direction is the easy axis when $K_u^{eff} > 0$.) These high, positive values for the effective PMA in our samples are comparable with the ones estimated in other Co/Ni(111) multilayers[16,19] and are related to the fact that, for ultrathin Co films, the interfacial anisotropy contribution is much stronger than the volume one.[16,33]

B. Magnetic domains imaging by Kerr microscopy

The presence and shape of magnetic domains was checked under application of an in-plane magnetic field by using polar Kerr microscopy. In Fig. 2, snapshots obtained for the sample with $t_{Co} = 0.20$ nm are shown; similar images were measured for all the other samples, with different values of cobalt thickness. The magnetic field was applied every 200 Oe and a 5-times averaging was performed for each image to reduce the noise. Bubble domains with magnetization perpendicular to the film plane are observed for in-plane field up to $H \approx 3.8$ kOe. At a fixed value of H, the shape and size of domains appear to be nearly the same for all the investigated samples. For small field, the domains shape is nearly circular with radius $r \approx 0.5 \times 10^{-4}$ cm. With increasing the field intensity, the radius seems not to change very much up to $H \approx 3$ kOe, when contrast starts decreasing. Eventually, for $H > H_C$, a uniform ground-state configuration with in-plane magnetization is realized.

C. Thermal spin waves measured by Brillouin light scattering

BLS measurements from thermally excited spin waves were performed in backscattering geometry at room temperature using a Sandercock-type (3 + 3)-pass tandem Fabry-Perot interferometer.[34] An in-plane magnetic field H was applied parallel to the sample surface and perpendicular to the plane of incidence of light. Light was focused onto the sample with an angle of incidence of 10°.

In Fig. 3 we show two representative BLS spectra, measured for the sample with $t_{Co} = 0.3$ nm at two different field values. The dependence of the frequency peaks on magnetic field applied in plane is displayed in Fig. 4 for various Co/Ni(111) multilayer samples, which differ only in the thickness of the Co layer t_{Co}, ranging between 0.15 and 0.35 nm, while $t_{Ni} = 0.6$ nm is fixed.

One observes a higher frequency mode which presents the typical field dependence of a film with a perpendicular magnetization: namely, a minimum at a critical field H_C, whose value depends on t_{Co}.[25,26] H_C coincides with the saturation field H_{sat} defined in the VSM loops. There is, however, an unprecedented feature that is worth noticing:

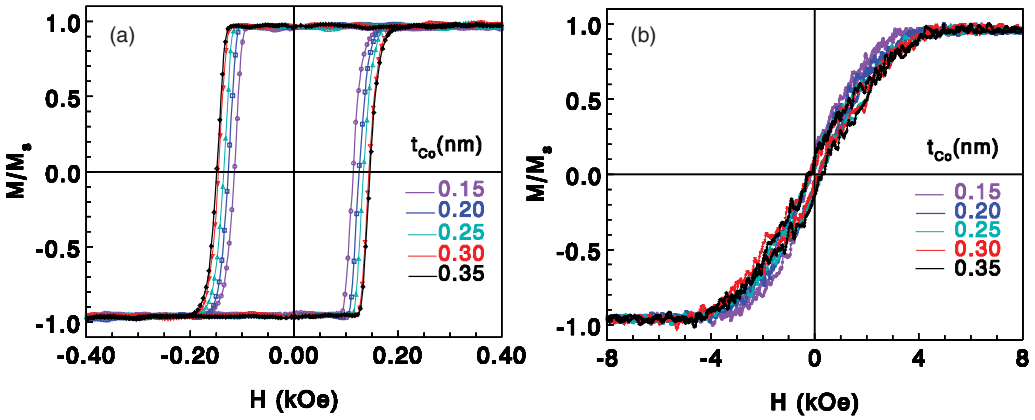

FIG. 1. (Color online) VSM hysteresis loops of Co/Ni multilayers, measured for magnetic field applied perpendicular (a) and parallel (b) to the film plane, respectively. Different cycles refer to samples with different values of cobalt thickness, t_{Co}, ranging between 0.15 and 0.35 nm, while nickel thickness is fixed ($t_{Ni} = 0.6$ nm).

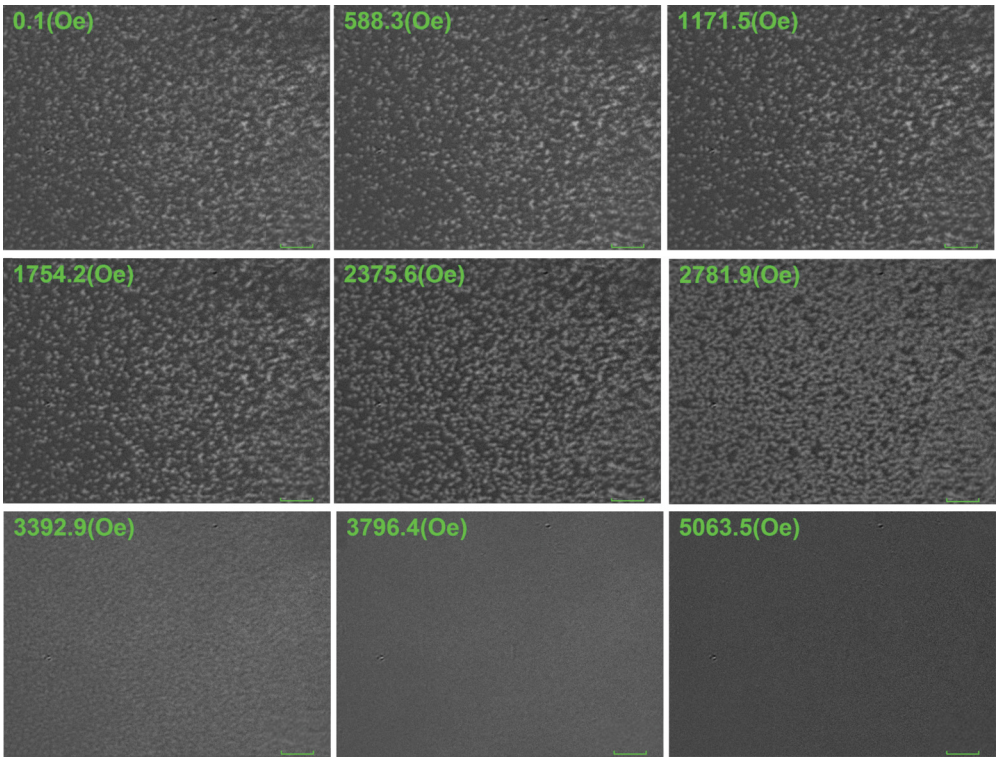

FIG. 2. (Color online) Snapshots of polar Kerr microscopy images, obtained for different values of the magnetic field, H, applied in the plane of a Co/Ni(111) multilayer sample with $t_{Co} = 0.20$ nm. The scale bar denotes 10 μm and applies at all frames. Bubble domains with magnetization perpendicular to the film plane can be clearly observed for $|H| < 3$ kOe and fade out at ≈3.8 kOe.

a nonmonotonic dependence of the spin-wave frequency *on cobalt thickness*. In fact, as one passes from $t_{Co} = 0.30$ nm to 0.35 nm, the zero field gap decreases, slightly but noticeably, and so does the critical field H_C.

Another, lower frequency mode ($\nu \approx 3$ GHz) is observed by BLS spectra in a limited range of magnetic fields between ≈2.5 kOe and H_C (see Fig. 4). For all samples, the mode frequency was found to decrease weakly with decreasing H. It is worth noticing that the presence, in the BLS spectra (see Fig. 3), of the high-intensity, elastic peak, centered at zero frequency, prevented us from observing the lower frequency mode for $H < 2.5$ kOe. The field dependence of this mode closely resembles the one observed years ago[29] by BLS in ultrathin Co/Au(111) films. In that system, the simultaneous occurrence of two modes below the critical field H_C was tentatively attributed[29] to the presence of two spin-wave modes with respect to a ground state with up/down stripe domains[35] (i.e., stripes with opposite values of the magnetization component perpendicular to the film plane). However, the field dependence of the lower-frequency mode in ultrathin Co/Au(111) films could not be reproduced by such a model and, in the absence of a direct observation of domains, it remained unexplained.[29] In the next section we show that, in the case of our Co/Ni(111) multilayers, the presence of a ground state with bubble domains can provide a possible explanation for the field dependence of the two modes observed in the BLS spectra.

As a final remark on the BLS experimental data, let us notice that the measured frequencies were independent of the in-plane direction of the spin-wave wave vector, reflecting the in-plane isotropy of the multilayers. In addition, the frequency evolution with the intensity of the applied field was reversible, that is, independent of the ascending or descending evolution of the field H, in agreement with the unhysteretic shape of the magnetization curves of Fig. 1(b).

III. THE MODEL

In order to interpret the experimental BLS data in our Co/Ni(111) multilayers, we start from a simplified model, capable of catching the essential features of the dynamics for not-too-high fields, when domains are present (see Fig. 2). It is worth noticing that, for films with thickness less than the exchange length (in practice, nm-thick magnetic films), the existence and stability of a domain phase in the presence of an in-plane field was thoroughly investigated some years ago by Baryakhtar and Ivanov.[36] They showed that the equilibrium domain structure is located at H about $H_u - 4\pi M_s$ (where $H_u = 2K_u/Ms$), being metastable at small fields. According to theory,[36] the phase transition from the uniform state to domains is of the first order, pointing to the formation of a bubble domain structure. In the case of our Co/Ni(111) multilayers with thickness in the nm range, bubblelike domains were indeed observed. For the sake of simplicity, even though the domains are not arranged in a periodic pattern (see Fig. 2), we assume a hexagonal bubble lattice, which has the advantage of being isotropic from the demagnetization energy point of view.[37] (The magnetostatic energy was shown[38,39] not to

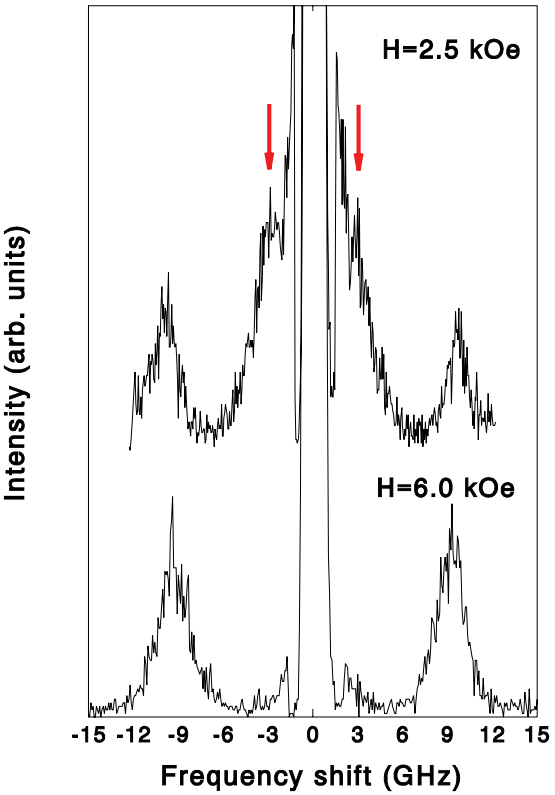

FIG. 3. (Color online) Two representative Brillouin light scattering spectra, measured for the sample with $t_{Co} = 0.3$ nm for two different field values. Arrows denote additional peaks measured for $H = 2.5$ kOe.

depend on the bubble lattice geometry, for high values of the ratio between the nearest-neighbor distance and the sample thickness; see discussion later on.) Each bubble is assumed to be a perfect cylinder of thickness t and radius r, while the mean distance between the centers of two nearest-neighbor bubbles (the lattice constant, in the case of a periodic pattern) is $a > 2r$. Inside the bubbles, the saturation magnetization M_s is directed along $+z$, the normal to the film plane, and is opposite to the region outside the bubbles.[40] The free energy density can be written[35,37]

$$G = G_u + G_D + G_Z + G_w, \tag{1}$$

where G_u is the uniaxial out-of-plane (i.e., perpendicular) anisotropy energy, G_D is the demagnetization energy of the domain lattice, G_Z is the Zeeman energy term due to an external magnetic field, and G_w is the energy of the wall between two domains with opposite magnetizations.

Due to the two opposite orientations of M_s, two spin-wave modes are expected to arise from $G_u + G_D + G_Z$. If a dc magnetic field, H, is applied in plane, the azimuthal angles of magnetization orientation in the two kinds of domains are $\theta_1 = \arcsin(H/H_C)$ and $\theta_2 = \pi - \theta_1$ for $H < H_C = H_u - 4\pi M_s N_{zz}$. The uniaxial effective field $H_u = 2K_u/M_s$ is defined in terms of the out-of-plane anisotropy constant K_u, and N_{zz} is the out-of-plane demagnetization factor associated with the domain pattern. The frequencies of the two spin-wave-excitation modes are readily calculated by the Smit-Beljers

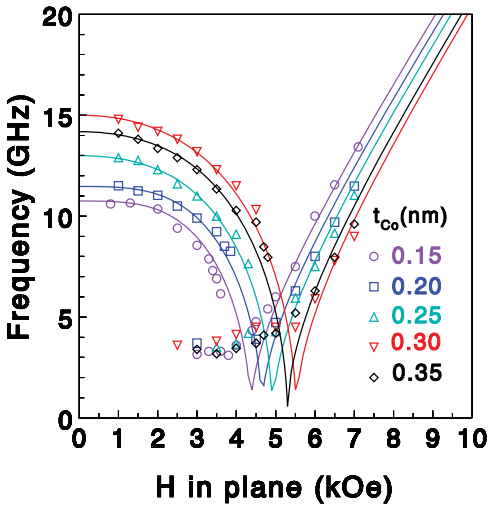

FIG. 4. (Color online) Dependence of the spin-wave frequency modes of the Co/Ni(111) multilayers, measured by BLS, on H, the intensity of a magnetic field applied in plane, for different values of t_{Co}, the Co thickness. Notice the nonmonotonic dependence of the higher frequency mode *on Co thickness*, as t_{Co} passes from 0.30 to 0.35 nm. Large open symbols, BLS data; continuous lines, calculations performed using Eq. (11).

procedure,[41] and for $H < H_C$ they turn out to be[37]

$$\left(\frac{\omega^+}{\gamma}\right)^2 = (H_C^2 - H^2) + \frac{4\pi M_s N_\parallel}{H_C}(H_C^2 + H^2),$$
$$\left(\frac{\omega^-}{\gamma}\right)^2 = (H_C^2 - H^2)\left(1 + \frac{4\pi M_s N_\parallel}{H_C}\right), \tag{2}$$

where γ is the gyromagnetic ratio. The frequencies ω^+ and ω^- can be interpreted as an acoustic and an optic mode, on the basis of the in-phase and out-of-phase precession, respectively, of the spin components perpendicular to the domain wall. Note that, in Eq. (2), one has $N_\parallel \equiv N_{xx} = N_{yy}$ in the hypothesis of isotropy within the film plane (e.g., valid for a hexagonal bubble lattice).[37] For $H \geqslant H_C$, the domain structure is wiped out and the film is uniformly in-plane magnetized ($\theta_1 = \theta_2 = \frac{\pi}{2}$); the optic mode ω^- vanishes, while the acoustic mode ω^+ evolves into the uniform mode ω_0,

$$\left(\frac{\omega_0}{\gamma}\right)^2 = H(H - H_u + 4\pi M_s), H \geqslant H_C. \tag{3}$$

In general, the demagnetization factors N_{xx}, N_{yy}, N_{zz} satisfy $N_{xx} + N_{yy} + N_{zz} = 1$ and, for a bubble domain lattice, their values depend on the domain aspect ratio $\rho = 2r/t$.[37] In the case of the Co/Ni(111) ultrathin multilayers under study, one has $t \approx 1$ nm; from direct domain observation by polar Kerr microscopy, one estimates $2r \approx 1$ μm. It follows $\rho \approx 10^3$, leading to $N_{zz} \approx 1$ and $N_\parallel \approx 0$. As a consequence, one expects that in Co/Ni(111) multilayers, the two spin-wave modes ω^+ and ω^-, which are exactly degenerate at zero field, should be hardly distinguishable even for $0 < H < H_C$ (see Fig. 5).

For $H < H_C$, besides the two spin-wave modes ω^+ and ω^-, the domains are expected to contribute to the spectrum of excitations with an additional mode which is associated with the "domain wall."[35,42–47] In fact, in Eq. (1) one should also consider G_w, the wall contribution to the free energy density,

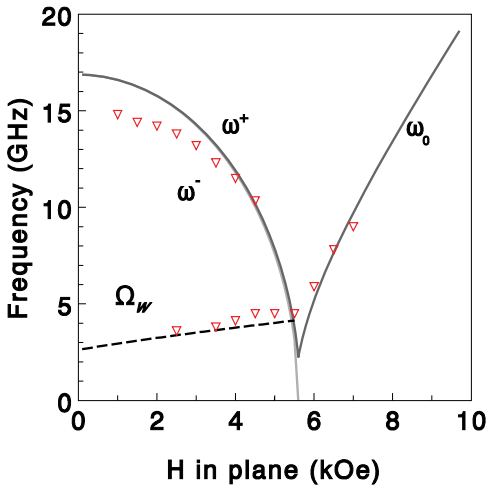

FIG. 5. (Color online) Field dependence of the domain wall oscillation frequency, Ω_w [Eq. (5), dashed line], calculated for a magnetic film with a bubble domain pattern of aspect ratio $\rho = 2r/t \approx 10^3$ (see text). For the same domain pattern, the calculated frequencies of the two spin-wave modes, ω^- and ω^+ [Eq. (2), full lines], turn out to be nearly degenerate for $H < H_C$. For $H \geqslant H_C$, the frequency of the uniform spin-wave mode ω_0 [Eq. (3), full line] is also shown. Experimental BLS data (open triangles) refer to a Co/Ni(111) multilayer sample with $t_{\mathrm{Co}} = 0.30$ nm.

which cannot be expressed in closed form. It is convenient[35] to separate G_w into a static term G_{w0} (whose minimization requires that domains with opposite magnetization have the same volume fraction) and a linearized dynamic term G_{w1} (which represents the kinetic energy of a moving domain wall). The wall can harmonically oscillate around its equilibrium position with angular frequency $\Omega_w = \sqrt{C/m_{\mathrm{eff}}}$, where C is a restoring force constant density and m_{eff} is an effective wall mass density.[35,42–47] For the Co/Ni(111) multilayer, this mechanism gives rise to a mode with frequency Ω_w, whose order of magnitude and field dependence are calculated in Sec. III A and turn out to be in fair agreement with the lower-frequency mode observed by BLS at $\nu \approx 3$ GHz. In Sec. III B, the frequency of the higher-energy mode, also observed by BLS, is calculated assuming $N_{zz} \approx 1$ and $N_{\parallel} \approx 0$ in the whole field range between 0 and H_C. Moreover, we include a second-order uniaxial out-of-plane anisotropy in the model, since such a contribution is known to be non-negligible in Co ultrathin films.[28,29]

A. Lower frequency mode

The lower frequency mode of the Co/Ni(111) multilayers can be interpreted as due to a collective mode of the domain walls, harmonically oscillating around their equilibrium positions in the bubble domain pattern, at an angular frequency

$$\Omega_w = \sqrt{\frac{C}{m_{\mathrm{eff}}}}, \tag{4}$$

where C (dyne/cm^3) is a restoring force density and m_{eff} (g/cm^2) is an effective wall mass density. The restoring force acting on the domain wall is determined by the shape of domains and the magnetostatic energy of the system.[37,44,46] The inertia of a domain wall is not associated with a real mass: It arises because the profile of a moving wall is slightly altered with respect to the static one. Consequently, the moving wall is associated with an increase in the dipolar energy, which can be shown to have the form of a kinetic energy.[35,42–46]

Both C and m_{eff} are expected to be modified by the application of an external field in the film plane, according to

$$\Omega_w = \sqrt{\frac{C_0}{m_0}}\sqrt{\frac{1-(H/H_C)^2}{m^*(H)}}. \tag{5}$$

C_0 and m_0 denote the zero-field restoring force and effective wall mass density, respectively; $m^*(H) = m_{\mathrm{eff}}(H)/m_0$ is defined as the ratio between the field-dependent effective mass density of the wall, $m_{\mathrm{eff}}(H)$, and m_0.

Concerning the restoring force density, its zero-field value takes the form, in the case of a hexagonal bubble lattice,[37,44,46]

$$C_0 = \frac{8\pi M_s^2}{r}\Bigg\{-1+4\sqrt{3}\pi\left(\frac{r}{a}\right)^2 + \frac{8\pi r^3}{\sqrt{3}ta^2}\sum_{\mathbf{K}\neq 0}(Kr)^{-2}(1-e^{-tK}) \times\left[KrJ_0^2(Kr)+J_0(Kr)J_1(Kr)-KrJ_1^2(Kr)\right]\Bigg\}. \tag{6}$$

The summation is carried over all of the distinct vectors $\mathbf{K}$ of the reciprocal lattice, and the argument of the Bessel functions of order 0 and 1 is $Kr = 2\pi\frac{r}{a}\sqrt{n_1^2+\frac{1}{3}n_2^2}$, where the integers n_1 and n_2 are not simultaneously zero. In Eq. (5), the analytic field dependence of the restoring force density is clearly a consequence of its magnetostatic origin: $C(H) \propto M_s^2\cos^2\theta_1 \propto M_s^2[1-(H/H_C)^2]$.

Concerning the effective wall mass density, its zero-field value was first estimated by Döring[42] to be $m_0 = 1/(2\pi\gamma^2\Delta)$; $\Delta = \sqrt{A_{\mathrm{exch}}/K_u}$ is the domain wall width, expressed as the ratio between the exchange stiffness constant, A_{exch} (erg/cm), and the perpendicular anisotropy constant, K_u (erg/cm^3). In general, the calculation of the field-dependent ratio $m^*(H) = m_{\mathrm{eff}}(H)/m_0$ has to be performed numerically [see Eq. (7) below];[35,43–46,48,49] closed form expressions of $m^*(H)$ are available[46] only for materials with $Q = \frac{H_u}{4\pi M_s} \gg 1$.

The material parameters of Co/Ni(111) films were deduced from experimental VSM and polar Kerr microscopy data: For example, for a sample with $t_{\mathrm{Co}} = 0.3$ nm, saturation field $H_{\mathrm{sat}} \approx 5.5$ kOe, and saturation magnetization $M_s \approx 780$ emu/cm^3, one has $H_u = 15.3$ kOe and $4\pi M_s = 9.8$ kOe, corresponding to $Q = 1.56$. Using $r = 0.5\times10^{-4}$ cm, $a = 3\times10^{-4}$ cm, $A_{\mathrm{exch}} = 1\times10^{-6}$ erg/cm, and $\gamma/(2\pi) \approx 3$ GHz/kOe,[50] for a film with $t = 1\times10^{-7}$ cm, the correct order of magnitude of the domain wall oscillation frequency in zero field is obtained: $\nu_0 = \frac{1}{2\pi}\sqrt{\frac{C_0}{m_0}} \approx 2.7$ GHz. For high values of the ratio between the nearest-neighbor distance, a, and the sample thickness, t, the magnetostatic energy was shown not to depend on the bubble lattice geometry.[38,39] Thus, even for an amorphous bubble array, we expect the frequency ν_0 to be not very different from the previous value (calculated for a regular hexagonal lattice of bubbles), provided that a is interpreted as the mean distance between two bubbles. Concerning the field dependence of the frequency, we have

numerically calculated the ratio between the effective mass density of the wall, $m_{\rm eff}(H)$, and the zero-field (Döring) mass, m_0, using the expression[35,48]

$$m^*(H) = \frac{m_{\rm eff}(H)}{m_0} = \frac{1}{2}\int_{\theta_1}^{\pi-\theta_1} \frac{\sin x}{h+\sin x} \times \sqrt{\sin^2 x - \sin^2\theta_1 - 2\mu(\sin x - \sin\theta_1)}\,dx, \quad (7)$$

where $\mu = \frac{H}{H_u}$ and $h = \frac{H}{4\pi M_s}$ are reduced fields, and $\sin\theta_1 = \frac{H}{H_C}$. By inserting the calculated values of $m^*(H)$ into Eq. (5), we finally obtain (see Fig. 5, dashed line) a smooth, monotonic dependence of the domain wall oscillation frequency on the intensity of the in-plane field, in fair agreement with BLS data. It is worth noticing that, in principle, the theory predicts a dynamic signature of the presence of domains even for low fields. However, in spite of the clear observation of bubble domains for $H < 2.5$ kOe (see Fig. 2), the lower frequency mode could not be observed in this range. The reason is that, for such low field values, the lower frequency peak becomes rather broad (more than 1 GHz, as can be inferred from inspection of Fig. 3) and approaches too closely the high-intensity, elastic BLS line centered at zero frequency; thus, it cannot be resolved.

Finally we notice that, by the above model, one cannot separate the Co and Ni contributions; that is, the material parameters represent the whole multilayer.

B. Higher frequency mode

In order to interpret the cobalt thickness dependence of the higher frequency mode of the various Co/Ni(111) samples investigated by BLS, we make use of a simplified model where $N_{zz} = 1$ and $N_{\parallel} = 0$; that is, owing to the high aspect ratio of the domain pattern ($\rho \approx 10^3$), we neglect the small frequency difference between the modes ω^+ and ω^- for $H < H_C$ (see Fig. 5). Moreover, hybridization of the latter modes with the "domain wall" mode Ω_w (which is possible[35,45] in the neighborhood of H_C) will be neglected. Finally, with the aim of distinguishing the Co and Ni contributions to the magnetic behavior, we describe the multilayer by a simple model consisting only of two ferromagnetic layers:[51,52] a cobalt layer with thickness $t_{\rm Co}$ and saturation magnetization $M_{\rm Co}$, and a nickel layer with thickness $t_{\rm Ni}$ and saturation magnetization $M_{\rm Ni}$. The two layers are supposed to be in contact, coupled by a ferromagnetic interlayer interaction $J_{\rm ex} > 0$. When a dc magnetic field H is applied in plane, for example, along y, the free energy of the system per unit area can be written as[51,52]

$$\begin{aligned} E = {} & t_{\rm Co}\big(K^{(1)}_{u,\rm Co}\sin^2\theta_{\rm Co} + K^{(2)}_{u,\rm Co}\sin^4\theta_{\rm Co} \\ & - H M_{\rm Co}\sin\theta_{\rm Co}\sin\phi_{\rm Co}\big) \\ & + t_{\rm Ni}\big(K^{(1)}_{u,\rm Ni}\sin^2\theta_{\rm Ni} - H M_{\rm Ni}\sin\theta_{\rm Ni}\sin\phi_{\rm Ni}\big) \\ & - J_{\rm ex} M_{\rm Co} M_{\rm Ni}[\cos\theta_{\rm Co}\cos\theta_{\rm Ni} \\ & + \sin\theta_{\rm Co}\sin\theta_{\rm Ni}\cos(\phi_{\rm Co} - \phi_{\rm Ni})]. \end{aligned} \quad (8)$$

$K^{(1)}_{u,\rm Co}$ and $K^{(2)}_{u,\rm Co}$, respectively, denote the first- and second-order uniaxial out-of-plane anisotropy constants of cobalt. Notice that $K^{(1)}_{u,\rm Co}$ is, indeed, a net perpendicular anisotropy, since it includes the negative contribution of shape anisotropy. The magnetization $M_{\rm Co}$ is supposed to form an angle $\theta_{\rm Co}$ with z, the normal to the film plane, while its projection on the film plane forms an angle $\phi_{\rm Co}$ with the x direction. It is useful to introduce effective magnetic fields associated with the first- and second-order anisotropy constants: $H^{(1)}_{u,\rm Co} = 2K^{(1)}_{u,\rm Co}/M_{\rm Co}$ and $H^{(2)}_{u,\rm Co} = 4K^{(2)}_{u,\rm Co}/M_{\rm Co}$. Similar definitions hold for the nickel layer, except that we set $K^{(2)}_{u,\rm Ni} = 0$ (see later). The strength of the interlayer ferromagnetic coupling can be measured conveniently by a symmetrized parameter,[51,52] which has the dimension of a magnetic field, $H_{\rm ex} = J_{\rm ex}\sqrt{M_{\rm Co}M_{\rm Ni}}/\sqrt{t_{\rm Co}t_{\rm Ni}}$. In the limit of very strong interlayer ferromagnetic coupling (i.e., $H_{\rm ex} \gg H$, $H^{(1)}_{u,\rm Co}$, $H^{(2)}_{u,\rm Co}$, and $H^{(1)}_{u,\rm Ni}$), it can be shown[51,52] that $\theta_{\rm Co} = \theta_{\rm Ni} = \theta$, where θ is obtained solving the equation

$$H\cos\theta = H^{(1)}_{\rm Keff}\sin\theta\cos\theta + H^{(2)}_{\rm Keff}\sin^3\theta\cos\theta. \quad (9)$$

whereas, $\forall\ H$, one has $\phi_{\rm Co} = \phi_{\rm Ni} = \frac{\pi}{2}$. The effective magnetic anisotropy fields of first and second order in Eq. (9), $H^{(1)}_{\rm Keff}$ and $H^{(2)}_{\rm Keff}$, are expressed, in terms of the corresponding quantities for the Co and Ni layers, as[51,52]

$$H^{(1,2)}_{\rm Keff} = \frac{t_{\rm Co}M_{\rm Co}H^{(1,2)}_{u,\rm Co} + t_{\rm Ni}M_{\rm Ni}H^{(1,2)}_{u,\rm Ni}}{t_{\rm Co}M_{\rm Co} + t_{\rm Ni}M_{\rm Ni}} \quad (10)$$

(where, for the nickel layer, $H^{(2)}_{u,\rm Ni} = 0$). The frequency of spin-wave excitations with respect to the ground state (9) can be calculated, following Smit and Beljers,[41] in terms of the second derivatives of the free energy (8). In the limit of strong interlayer ferromagnetic coupling, it can be shown[51,52] that the spectrum of the excitations of the Co/Ni bilayer admits just one mode, whose angular frequency ω turns out to be independent of the exchange field $H_{\rm ex}$ and takes the form

$$\left(\frac{\omega}{\gamma_{\rm eff}}\right)^2 = \frac{H}{\sin\theta}\big[H\sin\theta + H^{(1)}_{\rm Keff}(1-2\sin^2\theta) + H^{(2)}_{\rm Keff}(3\sin^2\theta - 4\sin^4\theta)\big], \quad (11)$$

where θ is given by Eq. (9), and the effective gyromagnetic ratio $\gamma_{\rm eff}$ is defined by[51,52]

$$\frac{t_{\rm Co}M_{\rm Co} + t_{\rm Ni}M_{\rm Ni}}{\gamma_{\rm eff}} = \frac{t_{\rm Co}M_{\rm Co}}{\gamma_{\rm Co}} + \frac{t_{\rm Ni}M_{\rm Ni}}{\gamma_{\rm Ni}}. \quad (12)$$

It results that $\gamma_{\rm eff}/(2\pi) \approx 3$ GHz/kOe is nearly the same for all samples, because the gyromagnetic ratios of Co and Ni in sputtered Co/Ni multilayers are nearly equal (3.006 and 3.090 GHz/kOe, respectively).[50] For the sake of simplicity, in the spin-wave frequency calculations we assumed bulk values, $M_{\rm Co} = 1400$ emu/cm^3 and $M_{\rm Ni} = 485$ emu/cm^3; it should be noted, however, that a somewhat smaller (15 %) value for $M_{\rm Ni}$ has been reported in the literature[50] for sputtered Ni multilayers with $t_{\rm Ni} = 50$ nm.

For the cobalt layer, with thickness $t_{\rm Co}$ in the range from 0.15 to 0.35 nm, both the first- and the second-order anisotropy constants, $K^{(1)}_{u,\rm Co}$ and $K^{(2)}_{u,\rm Co}$, were assumed to be positive in Eq. (8). The first-order anisotropy, $K^{(1)}_{u,\rm Co}$, turns out to be positive because, in such ultrathin layers, the strong out-of-plane interfacial anisotropy of Co/Ni(111)[16,33] and of Co/Pt(111)[53] overwhelm the easy-plane contribution from shape anisotropy. For example, for $t_{\rm Co} = 0.3$ nm, assuming a dipolar volume anisotropy $K_{d,\rm Co} = -2\pi M^2_{\rm Co} = -1.23\times10^7$ erg/cm^3, the estimated shape anisotropy

contribution is $t_{\mathrm{Co}}K_{d,\mathrm{Co}} = -0.37$ erg/cm^2, to be compared with positive values, for the interfacial anisotropy, as large as $K_s^{\mathrm{Co\text{-}Ni}} \approx 0.42$ erg/cm^2 and $K_s^{\mathrm{Co\text{-}Pt}} \approx 0.57$ erg/cm^2, taken from the literature on Co/Ni(111) multilayers.[16,33,53] The second-order anisotropy, $K^{(2)}_{u,\mathrm{Co}}$, is known to be non-negligible and positive according to previous experimental ferromagnetic resonance[54] and BLS[28,29] data in epitaxial Co films and sputtered Co/Ni(111) multilayers.[50]

In contrast, for the nickel layer with fixed thickness $t_{\mathrm{Ni}} = 0.6$ nm, we assumed $K^{(1)}_{u,\mathrm{Ni}} < 0$ and $K^{(2)}_{u,\mathrm{Ni}} = 0$. Actually, since in the multilayer model the interfacial anisotropy has been entirely attributed to the Co layer, one has to consider only the contribution from the dipolar volume anisotropy of nickel, $K^{(1)}_{u,\mathrm{Ni}} \approx K_{d,\mathrm{Ni}} = -2\pi M^2_{\mathrm{Ni}} = -0.148 \times 10^7$ erg/cm^3, which represents the leading term in the Ni total volume anisotropy, $K_{v,\mathrm{Ni}} = K_{d,\mathrm{Ni}} + K_{c,\mathrm{Ni}} + K_{e,\mathrm{Ni}}$. In fact, in sputtered ultrathin Ni/Pt multilayers with (111) texture and thicknesses comparable to ours,[55] both the magnetocrystalline volume anisotropy, $K_{c,\mathrm{Ni}}$, and the magnetoelastic volume anisotropy, $K_{e,\mathrm{Ni}}$, were found to be at least one order of magnitude smaller than $K_{d,\mathrm{Ni}}$; moreover, no evidence for the presence of a second-order anisotropy $K^{(2)}_{u,\mathrm{Ni}}$ was found.[55]

In Fig. 4, the experimental BLS data for the field dependence of the higher frequency mode are compared with theoretical curves, obtained from Eq. (11). Depending on the value of cobalt thickness, t_{Co}, in each Co/Ni(111) multilayer sample, the values of $K^{(1)}_{u,\mathrm{Co}}$ and $K^{(2)}_{u,\mathrm{Co}}$ were fitted in order to reproduce the zero-field gap, $\omega = \gamma_{\mathrm{eff}} H^{(1)}_{\mathrm{Keff}}$, as well as the critical field, $H_C = H^{(1)}_{\mathrm{Keff}} + H^{(2)}_{\mathrm{Keff}}$, above which the magnetization lies in plane ($\theta = \pi/2$). The so-obtained values for the first- and second-order net perpendicular anisotropy constants of the Co layer are reported in Table I. Both the order of magnitude of the anisotropies and their dependence on t_{Co} turn out to be similar to those measured by BLS in ultrathin Co/Au(111) films.[28,50,54] The systematic increase of Co anisotropies as t_{Co} decreases is due to the presence of the interfacial Co/Ni(111) and Co/Pt(111) anisotropies, favoring perpendicular orientation of the magnetization.[28] Moreover, in agreement with previous observations in similar systems,[28,50,54] we find that the inclusion of the second-order perpendicular anisotropy on the Co layer is necessary in order to obtain the good fit shown in Fig. 4 for the spin-wave frequency of our Co/Ni(111) multilayers.

TABLE I. The first- and second-order net perpendicular anisotropy constants, $K^{(1)}_{u,\mathrm{Co}}$ and $K^{(2)}_{u,\mathrm{Co}}$, of the Co layer as a function of its thickness, t_{Co}. The reported values were obtained using Eq. (11) to fit the BLS data in Fig. 4. Notice the nonmonotonic dependence of the effective anisotropy field of the multilayer, H_C, *on Co thickness*, as one passes from $t_{\mathrm{Co}} = 0.30$ to 0.35 nm. For $H \geqslant H_C$, the multilayer magnetization lies in plane. To calculate $H_C = H^{(1)}_{\mathrm{Keff}} + H^{(2)}_{\mathrm{Keff}}$ [see Eq. (10) and text], we assumed $H^{(1)}_{u,\mathrm{Ni}} = -6.1$ kOe and $H^{(2)}_{u,\mathrm{Ni}} = 0$, for the Ni layer with fixed thickness $t_{\mathrm{Ni}} = 0.6$ nm.

t_{Co} (nm)	$K^{(1)}_{u,\mathrm{Co}}$ (10^7 erg/cm^3)	$K^{(2)}_{u,\mathrm{Co}}$ (10^7 erg/cm^3)	$H^{(1)}_{u,\mathrm{Co}}$ (kOe)	$H^{(2)}_{u,\mathrm{Co}}$ (kOe)	H_C (kOe)
0.15	1.169	0.070	16.7	2.0	4.4
0.20	0.973	0.063	13.9	1.8	4.7
0.25	0.896	0.042	12.8	1.2	4.9
0.30	0.875	0.035	12.5	1.0	5.5
0.35	0.770	0.035	11.0	1.0	5.3

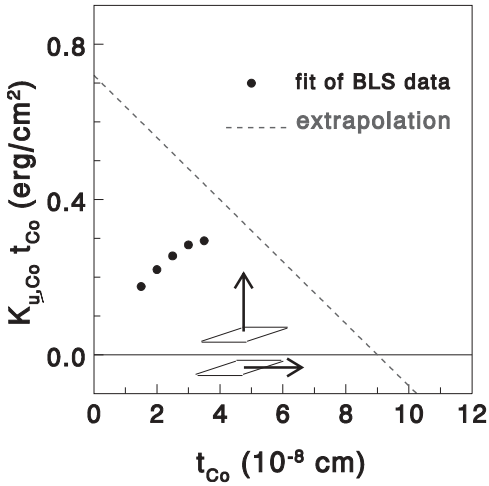

FIG. 6. Dependence on the Co layer thickness, t_{Co}, of the product $K_{u,\mathrm{Co}}t_{\mathrm{Co}}$, where $K_{u,\mathrm{Co}} = K^{(1)}_{u,\mathrm{Co}} + K^{(2)}_{u,\mathrm{Co}}$ is the effective perpendicular anisotropy of the Co layer in Co/Ni(111) multilayers. For $t_{\mathrm{Co}} > 3.5 \times 10^{-8}$ cm, a linear extrapolation (dashed line, see text) is proposed, which predicts the Co layer magnetization to become parallel to the film plane for t_{Co} greater than a critical value (9×10^{-8} cm), corresponding to ≈4.5 atomic layers.

Using the fitted values of the Co anisotropies reported in Table I, we calculated (see Fig. 6) the Co-thickness dependence of the product $K_{u,\mathrm{Co}}t_{\mathrm{Co}}$, where $K_{u,\mathrm{Co}} = K^{(1)}_{u,\mathrm{Co}} + K^{(2)}_{u,\mathrm{Co}}$ is the effective perpendicular anisotropy of Co in Co/Ni(111). One can guess the curve to have a maximum for $t_{\mathrm{Co}} \approx 3.5 \times 10^{-8}$ cm, and then follow a linear dependence, like the one displayed by a dashed line in Fig. 6: $K_{u,\mathrm{Co}}t_{\mathrm{Co}}$ (erg/cm^2)$= 0.72$–$0.80 t_{\mathrm{Co}}(10^{-8}$ cm). The vertical intercept and the negative slope represent, respectively, the effective interface anisotropy and the volume anisotropy of Co, in fair agreement with values reported in the literature.[16,33] A transition from out-of-plane to in-plane magnetization of the Co film is expected for $t_{\mathrm{Co}} > 9 \times 10^{-8}$ cm, again in agreement with former results in similar systems: Co/Ni(111) films,[16] Co/Au(111) films,[28] and Co/Pt(111) multilayers.[56] The feature of a deviation from the linear (Kt-versus-t) behavior at small thicknesses is often encountered in the anisotropy studies of transition-metal multilayers.[57] Several explanations can be given, the most likely being that, at small thicknesses, the Co layers become discontinuous or islandlike, yielding a lower effective interface area, and thus a lower interface contribution to the magnetic anisotropy.[57]

Now we are able to qualitatively account for the non monotonic dependence of the critical field H_C *on Co thickness*, see Fig. 4 and the last column in Table I. As a matter of fact, from the linear extrapolation in Fig. 6, one expects the effective anisotropy field of the cobalt layer, $H^{(1)}_{u,\mathrm{Co}} + H^{(2)}_{u,\mathrm{Co}}$, to decrease as t_{Co} increases, and eventually become negative for a Co thickness corresponding to ≈4.5 atomic layers. From Eqs. (10), a qualitatively similar behavior is expected also for the effective anisotropy fields of the Co/Ni(111)

multilayer, $H_{\mathrm{Keff}}^{(1)}$ and $H_{\mathrm{Keff}}^{(2)}$. Thus, one can estimate $t_{\mathrm{Co}} \approx 4.5$ atomic layers as an upper limit, in order to have out-of-plane orientation of the magnetization of the whole Co/Ni(111) multilayer. Previous magneto-optical Kerr effect studies of Co/Ni multilayers epitaxially grown on Au(111) led to similar conclusions: The out-of-plane orientation of the multilayer magnetization occurred for $t_{\mathrm{Co}} \leqslant 4$ atomic layers.[33]

IV. CONCLUSIONS

In this paper, we have studied sputtering-grown, (111)-textured Co/Ni ultrathin samples with variable cobalt thickness and fixed nickel thickness. The multilayers are characterized by a high PMA, as revealed by VSM measurements, which makes them interesting for spintronic applications.[24] For magnetic field applied in plane and smaller than a few kOe's, the simultaneous existence of two modes was found by BLS and connected with the presence of bubble domains, revealed by polar Kerr microscopy. The lower-frequency mode, with a weak field dependence, was related to the excitation of an oscillating mode of the domain wall. The higher-frequency mode, which displays the typical field behavior of a film with a perpendicular anisotropy, was interpreted as a nearly doubly degenerate mode (in the bubble array, quasidegeneracy is a consequence of the high aspect ratio between the mean radius of a bubble and film thickness). The latter data were interpreted using a simplified model of two ferromagnetic layers, strongly coupled by a ferromagnetic interlayer exchange, with a strong out-of-plane anisotropy, attributed to the Co layer owing to the high Co-Ni and Co-Pt interfacial anisotropies.[16,33] To obtain a good fit for the higher-frequency mode, a second-order contribution to the uniaxial out-of-plane magnetic anisotropy of Co had to be included, in agreement with previous results in similar multilayer systems.[28,29,50,54] By this model, also the unprecedented feature of a nonmonotonic dependence of the frequency of the higher mode *on cobalt thickness* could be finely reproduced. Such a nonmonotonic t_{Co} dependence of frequency indeed mirrors the nonmonotonic t_{Co} dependence of the effective magnetic anisotropy field of the composite multilayers under study. This proves that BLS, as a technique that allows local magnetic measurements, is a very sensitive tool for probing anisotropy, provided that the two kinds of magnetic layers in the system are properly modeled. We believe that the present interpretation of BLS data in Co/Ni(111) multilayers might be a useful starting point for a critical reconsideration of similar BLS experiments in film and multilayer systems where the presence of domains was hypothesized.[27–31] Also, the effect of different ground-state pattern geometries (stripes versus bubbles) on the field dependence of spin-wave excitations,[37] is an issue that is worth investigating experimentally (e.g., by BLS or ferromagnetic resonance, supplemented by magnetic domains imaging) in a more systematic way.

ACKNOWLEDGMENTS

We acknowledge S. Fukami, from NEC Corporation, for providing us with the multilayer samples, and A. Rettori, from the University of Florence, for fruitful discussions. Support from European Community 7th Framework Programme under Grant Agreement No. 228673 (MAGNONICS) is gratefully acknowledged.

[1] S. N. Piramanayagam, J. Appl. Phys. **102**, 011301 (2007).
[2] D. C. Ralph and M. D. Stiles, J. Magn. Magn. Mater. **320**, 1190 (2008).
[3] J. A. Katine and E. E. Fullerton, J. Magn. Magn. Mater. **320**, 1217 (2008).
[4] T. Koyama, G. Yamada, H. Tanigawa, S. Kasai, N. Ohshima, S. Fukami, N. Ishiwata, Y. Nakatani, and T. Ono, Appl. Phys. Express **1**, 101303 (2008).
[5] H. Tanigawa, T. Koyama, G. Yamada, D. Chiba, S. Kasai, S. Fukami, T. Suzuki, N. Ohshima, N. Ishiwata, Y. Nakatani *et al.*, Appl. Phys. Express **2**, 053002 (2009).
[6] D. Chiba, G. Yamada, T. Koyama, K. Ueda, H. Tanigawa, S. Fukami, T. Suzuki, N. Ohshima, N. Ishiwata, Y. Nakatani *et al.*, Appl. Phys. Express **3**, 073004 (2010).
[7] H. Tanigawa, K. Suemitsu, S. Fukami, N. Ohshima, T. Suzuki, E. Kariyada, and N. Ishiwata, Appl. Phys. Express **4**, 013007 (2011).
[8] T. Koyama, D. Chiba, K. Ueda, H. Tanigawa, S. Fukami, T. Suzuki, N. Ohshima, N. Ishiwata, Y. Nakatani, and T. Ono, Nat. Mater. **10**, 194 (2011).
[9] T. Koyama, D. Chiba, K. Ueda, H. Tanigawa, S. Fukami, T. Suzuki, N. Ohshima, N. Ishiwata, Y. Nakatani, and T. Ono, Appl. Phys. Lett. **98**, 192509 (2011).
[10] W. H. Rippard, A. M. Deac, M. R. Pufall, J. M. Shaw, M. W. Keller, S. E. Russek, G. E. W. Bauer, and C. Serpico, Phys. Rev. B **81**, 014426 (2010).
[11] S. M. Mohseni, S. R. Sani, J. Persson, T. N. Anh Nguyen, S. Chung, Y. Pogoryelov, and J. Akerman, Phys. Status Solidi RRL **5**, 432 (2011).
[12] M. A. Hoefer, T. J. Silva, and M. W. Keller, Phys. Rev. B **82**, 054432 (2010).
[13] B. A. Ivanov and A. M. Kosevich, Zh. Eksp. Teor. Fiz. **72**, 2000 (1977).
[14] A. M. Kosevich, B. A. Ivanov, and A. S. Kovalev, Phys. Rep. **194**, 117 (1990).
[15] G. H. O. Daalderop, P. J. Kelly, and F. J. A. den Broeder, Phys. Rev. Lett. **68**, 682 (1992).
[16] M. T. Johnson, J. J. de Vries, N. W. E. McGee, J. aan de Stegge, and F. J. A. den Broeder, Phys. Rev. Lett. **69**, 3575 (1992).
[17] P. J. H. Bloemen, W. J. M. de Jonghe, and F. J. A. den Broeder, J. Appl. Phys. **72**, 4840 (1992).
[18] P. J. H. Bloemen and W. J. M. de Jonghe, J. Magn. Magn. Mater. **116**, L1 (1992).
[19] S. Mangin, D. Ravelosona, J. A. Katine, M. J. Carey, B. D. Terris, and E. E. Fullerton, Nat. Mater. **5**, 210 (2006).
[20] D. Ravelosona, S. Mangin, Y. Lemaho, J. A. Katine, B. D. Terris, and E. E. Fullerton, Phys. Rev. Lett. **96**, 186604 (2006).
[21] D. Ravelosona, S. Mangin, Y. Henry, Y. Lemaho, J. A. Katine, B. D. Terris, and E. E. Fullerton, J. Phys. D **40**, 1253 (2007).
[22] S. Mangin, D. Ravelosona, Y. Henry, J. A. Katine, and E. E. Fullerton, AAPPS Bull. **18**, 41 (2008).

[23]S. Mangin, Y. Henry, D. Ravelosona, J. A. Katine, and E. E. Fullerton, Appl. Phys. Lett. **94**, 012502 (2009).
[24]S. Fukami, T. Suzuki, H. Tanigawa, N. Ohshima, and N. Ishiwata, Appl. Phys. Express **3**, 113002 (2010).
[25]B. Heinrich, K. B. Urquart, J. R. Dutcher, S. T. Purcell, J. F. Cochran, A. S. Arrott, D. A. Steigerwald, and W. F. Egelhoff, J. Appl. Phys. **63**, 3863 (1988).
[26]J. R. Dutcher, J. F. Cochran, I. Jacob, and W. F. Egelhoff, Phys. Rev. B **39**, 10430 (1989).
[27]J. V. Harzer, B. Hillebrands, R. L. Stamps, G. Guenterodt, C. D. England, and C. Falco, J. Appl. Phys. **69**, 2448 (1991).
[28]A. Murayama, K. Hyomi, J. E. Eickmann, and C. M. Falco, J. Appl. Phys. **82**, 6186 (1997).
[29]A. Murayama, K. Hyomi, J. E. Eickmann, and C. M. Falco, J. Magn. Magn. Mater. **198-199**, 72 (1999).
[30]G. Gubbiotti, G. Carlotti, M. G. Pini, P. Politi, A. Rettori, P. Vavassori, M. Ciria, and R. C. O'Handley, Phys. Rev. B **65**, 214420 (2002).
[31]G. Gubbiotti, G. Carlotti, M. Ciria, and R. C. O'Handley, IEEE Trans. Magn. **38**, 2649 (2002).
[32]G. Gubbiotti, L. Albini, S. Tacchi, G. Carlotti, R. Gunnella, and M. De Crescenzi, Phys. Rev. B **60**, 17150 (1999).
[33]M. Gottwald, S. Girod, S. Andrieu, and S. Mangin, IOP Conf. Ser.: Mater. Sci. Eng. **12**, 012018 (2010).
[34]G. Carlotti and G. Gubbiotti, Riv. Nuovo Cimento **22**, 1 (1999).
[35]M. Ramesh and P. E. Wigen, J. Magn. Magn. Mater. **74**, 123 (1988).
[36]V. G. Baryakhtar and B. A. Ivanov, Sov. Phys. JETP **45**, 789 (1977).
[37]J. O. Artman and S. H. Charap, J. Appl. Phys. **49**, 1587 (1978).
[38]D. J. Craik, P. V. Cooper, and W. F. Druyvesteyn, Phys. Lett. A **34**, 244 (1971).
[39]P. V. Cooper and D. J. Craik, J. Phys. D: Appl. Phys. **6**, 1393 (1973).
[40]M. H. H. Hoefelt, J. Appl. Phys. **44**, 414 (1973).
[41]J. Smit and H. G. Beljers, Philips Res. Rep. **10**, 113 (1955).
[42]W. Doering, Z. Naturforsch. **3**, 373 (1948).
[43]J. C. Slonczewski, Int. J. Magn. **2**, 85 (1972).
[44]B. E. Argyle, W. Jantz, and J. C. Slonczewski, J. Appl. Phys. **54**, 3370 (1983).
[45]J. Morkowski, H. Doetsch, P. E. Wigen, and R. J. Yeh, J. Magn. Magn. Mater. **25**, 39 (1981).
[46]J. Morkowski and P. E. Wigen, J. Appl. Phys. **52**, 2344 (1981).
[47]U. Ebels, L. Buda, K. Ounadjela, and P. E. Wigen, Phys. Rev. B **63**, 174437 (2001).
[48]M. Ramesh, L. Pust, and P. E. Wigen, J. Magn. Magn. Mater. **54**, 1205 (1986).
[49]S. Batra and P. E. Wigen, J. Appl. Phys. **61**, 4207 (1987).
[50]J.-M. L. Beaujour, W. Chen, K. Krycka, C.-C. Kao, J. Z. Sun, and A. D. Kent, Eur. Phys. J. B. **59**, 475 (2007).
[51]A. Layadi and J. O. Artman, J. Magn. Magn. Mater. **92**, 143 (1990).
[52]A. Layadi, J. Appl. Phys. **83**, 3738 (1998).
[53]Z. Zhang, P. E. Wigen, and S. S. P. Parkin, J. Appl. Phys. **69**, 5649 (1991).
[54]C. Chappert, K. L. Dang, P. Beauvillain, H. Hurdequint, and D. Renard, Phys. Rev. B **34**, 3192 (1986).
[55]S.-C. Shin, G. Srinivas, Y.-S. Kim, and M.-G. Kim, Appl. Phys. Lett. **73**, 393 (1998).
[56]W. B. Zeper, F. J. A. M. Greidanus, P. F. Carcia, and C. R. Fincher, J. Appl. Phys. **65**, 4971 (1989).
[57]M. T. Johnson, P. J. H. Bloemen, F. J. A. den Broeder, and J. J. de Vries, Rep. Prog. Phys. **59**, 1409 (1996).